Seismic loss estimation based on end-to-end simulation

M. Muto, S. Krishnan, & J.L. Beck
California Institute of Technology, Pasadena, California

J. Mitrani-Reiser
Johns Hopkins University, Baltimore, Maryland

ABSTRACT: Recently, there has been increasing interest in simulating all aspects of the seismic risk problem, from the source mechanism to the propagation of seismic waves to nonlinear time-history analysis of structural response and finally to building damage and repair costs. This study presents a framework for performing truly "end-to-end" simulation. A recent region-wide study of tall steel-frame building response to a M_w 7.9 scenario earthquake on the southern portion of the San Andreas Fault is extended to consider economic losses. In that study a source mechanism model and a velocity model, in conjunction with a finite-element model of Southern California, were used to calculate ground motions at 636 sites throughout the San Fernando and Los Angeles basins. At each site, time history analyses of a nonlinear deteriorating structural model of an 18-story steel moment-resisting frame building were performed, using both a pre-Northridge earthquake design (with welds at the moment-resisting connections that are susceptible to fracture) and a modern code (UBC 1997) design. This work uses the simulation results to estimate losses by applying the MDLA (Matlab Damage and Loss Analysis) toolbox, developed to implement the PEER loss-estimation methodology. The toolbox includes damage prediction and repair cost estimation for structural and non-structural components and allows for the computation of the mean and variance of building repair costs conditional on engineering demand parameters (i.e. inter-story drift ratios and peak floor accelerations). Here, it is modified to treat steel-frame high-rises, including aspects such as mechanical, electrical and plumbing systems, traction elevators, and the possibility of irreparable structural damage. Contour plots of conditional mean losses are generated for the San Fernando and the Los Angeles basins for the pre-Northridge and modern code designed buildings, allowing for comparison of the economic effects of the updated code for the scenario event. In principle, by simulating multiple seismic events, consistent with the probabilistic seismic hazard for a building site, the same basic approach could be used to quantify the uncertain losses from future earthquakes.

1 INTRODUCTION

Advances in computational seismology and earthquake engineering allow for increasingly sophisticated predictions of seismic response of buildings, including end-to-end simulation (Krishnan et al. 2006a, 2006b). However, for these methods to be of value to decision-makers, they need to be translated into financial terms.

Seismologists have created 3-D Earth models, and with advances in parallel computing can simulate global and regional seismic wave propagation using Finite Element and Finite Difference methods. Similarly, advances in the finite-element modeling of structures now make it possible to produce three-dimensional models of tall buildings which capture many of the material and geometric nonlinearities associated with strong seismic loading, and to facilitate the modeling of structural stability and damage.

As these computational tools in seismology and structural engineering become more accurate, and the increasing availability of computational power makes the application of these tools on a large scale feasible, there exists an opportunity to use these tools to perform so called "end-to-end" earthquake simulations, modeling the process from the rupture physics to structural performance and economic loss. This approach in particular has the potential to be a very powerful tool for performance-based earthquake engineering (PBEE).

The Pacific Earthquake Engineering Center (PEER) has developed a modular approach for PBEE (Porter 2003; Moehle and Deierlein 2004; Goulet et al. 2007). The first step is a seismic hazard analysis for a site, to establish an intensity measure (IM) for potential ground motions. The second step is a structural analysis, in which the IM and structural design are used to determine the re-

sulting values for structural response measures such as peak transient inter-story drift ratio (IDR) or peak floor acceleration, which are referred to as engineering demand parameters (EDP). In the damage analysis phase, the EDP is used with experimentally or empirically determined fragility functions to compute damage measures (DM) for the building components. Finally, the DM values are used in a loss analysis, where the losses are calculated using measures such as repair cost, repair duration, and loss of life. The modules are designed to implement a probabilistic approach to hazard analysis, so that the final result is essentially an integral involving a set of conditional probability density functions, which are used to "integrate out" the uncertainties associated with each module.

In the PEER methodology, the first two steps are usually carried out using probabilistic seismic hazard and building vulnerability curves. Here, a full seismic risk analysis is not attempted; instead, only the damage and loss steps are implemented by applying an extended version of the MDLA toolbox developed at Caltech (Mitrani-Reiser 2007) to the results of a Southern California-wide study of the response of two steel-frame buildings to a M_w 7.9 scenario earthquake (Krishnan et al. 2006a, 2006b). This effectively extends the PBEE methodology to include simulation of the source rupture mechanism and wave propagation to the building site. Only one scenario event is considered here but work is underway to combine the results presented here with a probabilistic seismic hazard analysis to quantify uncertain losses from future earthquakes and hence, ultimately, to life-cycle costs for a building at one of the sites in the Southern California region.

2 SCENARIO EARTHQUAKE AND BUILDING RESPONSE

The regions of interest for this study are the Los Angeles basin and the San Fernando valley, areas with large inventories of high-rise buildings and high levels of seismic risk. The chosen scenario event is a M_w 7.9 earthquake along a 290-km segment of the southern San Andreas fault (similar to the 1857 Fort Tejon earthquake), with the slip model derived from a finite-source inversion of the November 3, 2002 Denali earthquake in Alaska (Ji et al. 2003). The rupture was initiated at Parkfield in central California, propagated in a south-easterly direction, and terminated just north of the San Gabriel valley, as shown in Figure 1 (inset). Krishnan et al. (2006a, 2006b) computed ground motion time histories for the 636 analysis sites (spaced uniformly at approximately 3.5 km, as shown in Figure 1) using the spectral element method (e.g. Komatitsch and Tromp 1999), with peak velocities of up to 2 m/s and peak displacements of about 2 m.

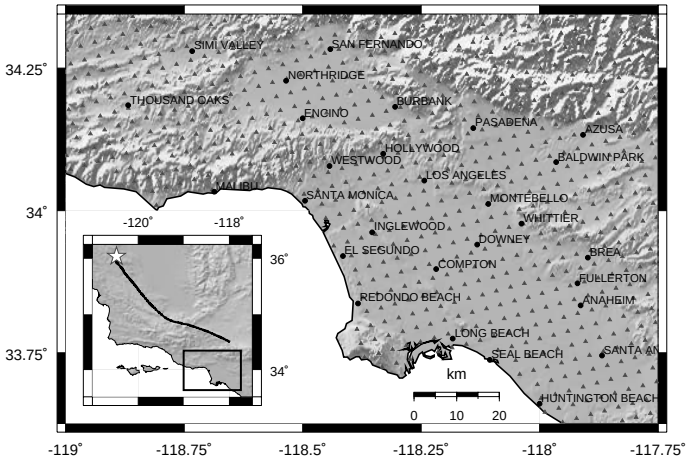

Figure 1. Scope of study area. Small triangles indicate locations where ground motion time histories are computed. Major cities are shown for reference. The inset shows the rupture trace in relation to the study area and the star represents the rupture initiation point (Parkfield).

At each analysis site, they performed three-dimensional nonlinear dynamic analyses of two building models using the program FRAME3D (Krishnan 2003; Krishnan and Hall 2006a, 2006b). Building response time histories were calculated, in addition to the induced structural damage, for two building designs.

Building 1 is based on an existing 18-story steel moment frame building, designed according to the 1982 Uniform Building Code (UBC) and constructed in 1986-87, that experienced significant damage (moment-frame connection fractures) during the 1994 Northridge earthquake. The existing building has 17 office stories above ground and a mechanical penthouse on top. The height above ground is 75.7 m. The typical floor plan is shown in Figure 2. The lateral force-resisting system consists of two-bay welded steel moment frames, two in each direction. The location of the north frame at one bay inside the perimeter results in some torsional eccentricity. Many of the moment-frame connections in the building fractured during the 1994 Northridge earthquake, leading to extensive studies of the building (SAC 1995; Carlson 1999). The finite-element model was developed from the building plans, and the material properties were based on samples of the structural steel from the building. The brittle failure of moment connections is also modeled in a probabilistic manner.

Building 2 uses the same architecture as Building 1, but the lateral force-resisting system has been redesigned according to the 1997 UBC. It has greater redundancy and strength than Building 1, with eight moment-frame bays in each direction (Figure 3). Additionally, moment connections designed after the 1994 Northridge earthquake are expected to behave in a ductile fashion, so connection fractures are not included in the analysis of Building 2.

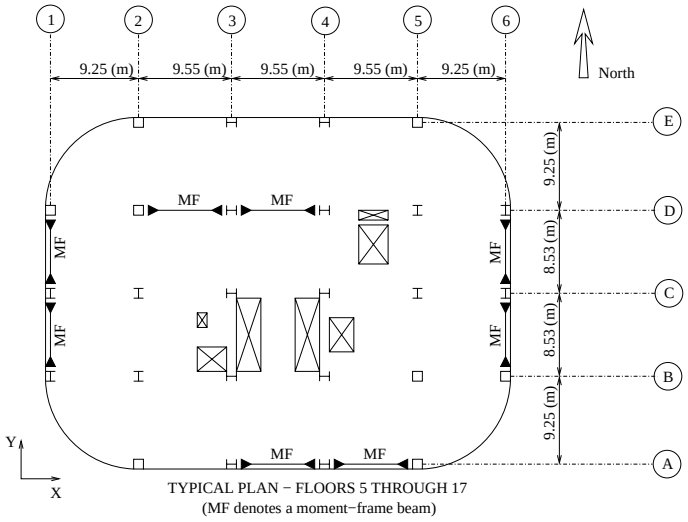

Figure 2. Typical plan for Building 1. Lines marked with `MF' indicate moment-frame bays.

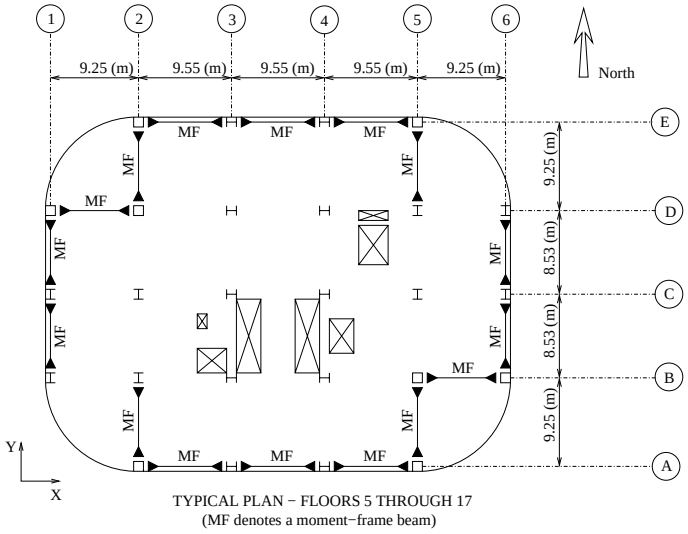

Figure 3. Typical plan for Building 2. Lines marked with `MF' indicate moment-frame bays.

Detailed floor plans, beam and column sizes, and gravity, wind, and seismic loading criteria for both buildings are given in Krishnan et al. (2005).

Values of peak IDR from the nonlinear analyses of the Buildings 1 and 2, subjected to the simulated ground motion time histories, are summarized in Figures 4 and 5, respectively. Shading is used to indicate building performance levels defined by FEMA 356 (2000) for Immediate Occupancy (IO), Life Safety (LS), and Collapse Prevention (CP). In addition to these performance categories, we classify buildings with greater damage as being Red-Tagged (RT) or Collapsed (CO). The peak IDR for Building 1 exceeds 0.05, the maximum value for performance level CP, throughout the San Fernando valley and in a major portion of the Los Angeles basin. For Building 2, values of peak IDR are reduced in the Los Angeles basin (but still exceed the maximum value for performance level LS of 0.025), and exceed 0.05 for most of the San Fernando valley.

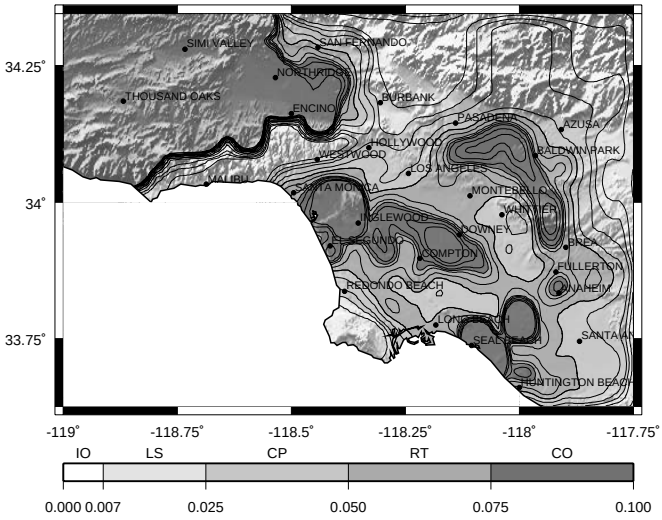

Figure 4. Peak IDR for Building 1 in the scenario earthquake, with regions classified according to FEMA limits for Immediate Occupany (IO), Life Safety (LS), and Collapse Prevention (CP), and two additional damage states, Red-Tagged (RT) and Collapsed (CO).

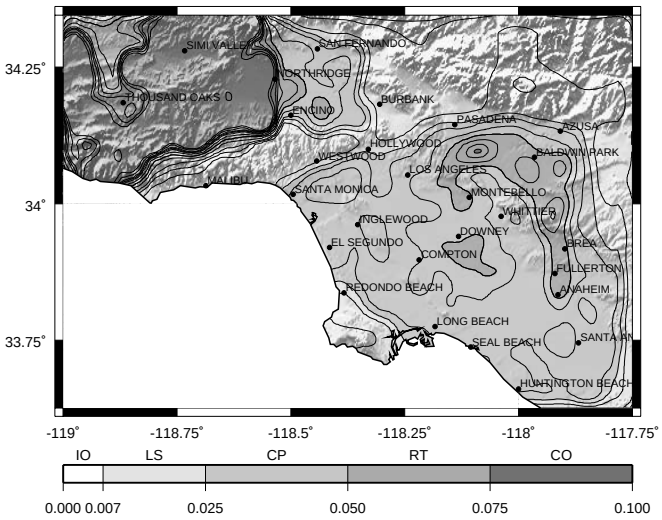

Figure 5. Peak IDR for Building 2 in the scenario earthquake, with regions classified according to FEMA limits for Immediate Occupany (IO), Life Safety (LS), and Collapse Prevention (CP), and two additional damage states, Red-Tagged (RT) and Collapsed (CO).

3 BASIS FOR LOSS ESTIMATION

While it has been demonstrated that for smaller events, damage to non-structural components can contribute significantly to life-cycle costs (e.g. Goulet et al. 2007), in large seismic events such as the one considered in this study, there is a significant probability for a building to suffer irreparable damage or even complete collapse.

Iwata et al. (2006) present a study of twelve steel structures damaged in the 1995 Kobe earthquake. Using the measured residual peak IDR and reported repair costs, they estimate a reparability limit of 0.015 for the peak residual IDR. However, there are two cases presented by Iwata et al. (2006) where buildings with peak residual IDR greater than 0.02 were successfully repaired. Based on this descrip-

tion, we chose to describe the probability of irreparable damage as a lognormal cumulative distribution function (CDF) parameterized with logarithmic median μ=0.02, and logarithmic standard deviation β=0.5. The cost of replacing Building 1 or 2 with a current state-of-the-art structure is estimated to be approximately $72 M (U.S.), including the cost of structural and non-structural components, and plumbing, electrical, and heating, ventilation and air-conditioning (HVAC) systems; the latter costs are based on estimates for current construction, as shown in the first part of Table 1.

The MDLA toolbox estimates repair costs using an assembly-based vulnerability approach (Porter 2000). The second part of Table 1 summarizes the damageable components in the buildings. In Building 1, damage to moment connections takes the form of connection fractures, which are calculated directly during the finite-element analysis. In Building 2, the moment connections are assumed to remain ductile. However, for large inter-story drifts, connections are expected to fail in a local flange-buckling mode. Since this mode of failure is not incorporated in the structural analysis, damage to connections for Building 2 is modeled using a probabilistic approach. The connections are grouped by story (e.g. connections at the second floor are associated with the first story) and direction of the moment-frame bay, and damage to each group is estimated using a fragility function based on the peak transient IDR at each story in the same direction as the connection group. This function is defined by a lognormal CDF with μ=0.05 and β=0.5. Probabilistic descriptions of damage to the interior partitions, exterior glazing, acoustical ceiling, and sprinkler system are calculated using fragility functions developed by Porter (2000) that have the form of lognormal CDFs. The governing EDP and fragility function parameters are summarized in the second part of Table 1.

Fragility functions for hydraulic elevators are given by Porter (2007). However, there is little published information on the repair and replacement of the traction elevators used in high-rise buildings. Following the Northridge earthquake, the elevators in Building 1 were unable to properly function due to approximately six inches of permanent roof displacement. Based on the observed damage pattern, a major portion of this displacement was most likely accommodated over four stories, resulting in a peak permanent IDR of 0.01. Therefore, the fragility function for the elevators is taken as a lognormal CDF on residual peak IDR with μ=0.01 and β=0.25. The plumbing, electrical, and HVAC systems are assumed to be robust, since we felt that serious damage to these components would likely be associated with irreparable structural damage, in which case the entire building must be replaced anyway.

Repair and replacement costs for components are also shown in Table 1. Average repair costs for the fractured moment connections in Building 1 are based on a collection of reported values for repairs to fractured connections in steel moment-frame buildings following the 1994 Northridge earthquake (Bonowitz and Maison 2003). Since a major portion of the cost is related to accessing the connection, which will be necessary for both fracture and local flange buckling, the cost for repair for both modes of failure is taken to be the same. Repair and replacement costs for the interior partitions, interior paint, exterior glazing, acoustical ceiling tiles, and sprinklers are given by Porter (2000).

Table 1. Repair/Replacement costs and fragility functions for building components.

Assembly	unit	Quantity	EDP	Fragility Parameters		Action	Cost
				μ	β		($ U.S.)
Structure in irreparable state							
Structure and cladding	ft^2	280,988	Perm. IDR	0.02	0.5	Replace	120
Plumbing systems	ft^2	280,988	Perm. IDR	0.02	0.5	Replace	5
Electrical systems	ft^2	280,988	Perm. IDR	0.02	0.5	Replace	10
HVAC	ft^2	280,988	Perm. IDR	0.02	0.5	Replace	20
Elevators	ea	3	Perm. IDR	0.02	0.5	Replace	1,000,000
Non-structural elements	ft^2	280,988	Perm. IDR	0.02	0.5	Replace	50
Construction costs	ft^2	280,988	Perm. IDR	0.02	0.5	Replace	40
Total cost							71,840,000
Structure in a reparable damage state							
Moment conn. (Bldg. 1; fracture mode)	ea	284	Damage calculated in FEA			Repair	20,000
Moment conn. (Bldg. 2; flange buckling)	ea	550	IDR	0.05	0.5	Repair	20,000
Drywall partitions (visible damage)	64 ft^2	6,098	IDR	0.0039	0.17	Repair	88
Drywall partitions (significant damage)	64 ft^2	6,098	IDR	0.0085	0.23	Repair	525
Drywall finish (visible damage)	64 ft^2	6,098	IDR	0.0039	0.17	Repair	88
Drywall finish (significant damage)	64 ft^2	6,098	IDR	0.0085	0.23	Repair	253
Exterior glazing	panel	3,423	IDR	0.040	0.36	Repair	439
Elevators	ea	3	Perm. IDR	0.01	0.25	Replace	1,000,000
Automatic sprinklers	12 ft	2,757	Accel.	32	1.4	Repair	900
Acoustical ceiling	ft^2	280,988	Accel.	92/(l+w)	0.81	Repair	2.21
Interior paint	ft^2	280,988	Based on ratio of dmg. to undmg. area			Repair	1.52

4 ESTIMATION OF REPAIR/REPLACEMENT COSTS FOR BUILDINGS UNDER THE SCENARIO EARTHQUAKE

To estimate the losses in Buildings 1 and 2 from the scenario earthquake, the EDPs (peak transient IDR, peak residual IDR, peak floor acceleration) obtained from Krishnan et al. (2006a, 2006b), are used with the fragility and repair/replacement cost functions summarized in Section 3. The geographical distribution of mean (expected) losses for Building 1 is shown in Figure 6. The building performs poorly, with complete losses for locations throughout the San Fernando valley and much of the Los Angeles basin. The performance of Building 2, shown in Figure 7, is much better; the predicted impact of the scenario earthquake in the Los Angeles basin is considerably lower than for Building 1, though significant losses are predicted in some areas of the San Fernando valley.

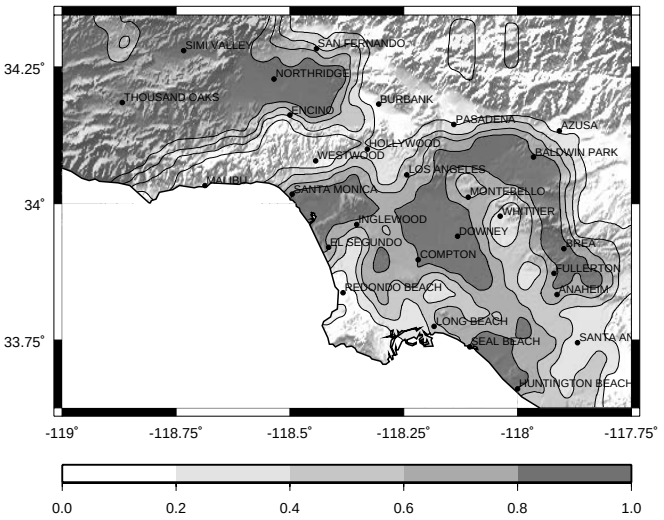

Figure 6. Mean loss for Building 1, normalized by building replacement cost. Near-total losses are calculated for the San Fernando valley and much of the Los Angeles basin.

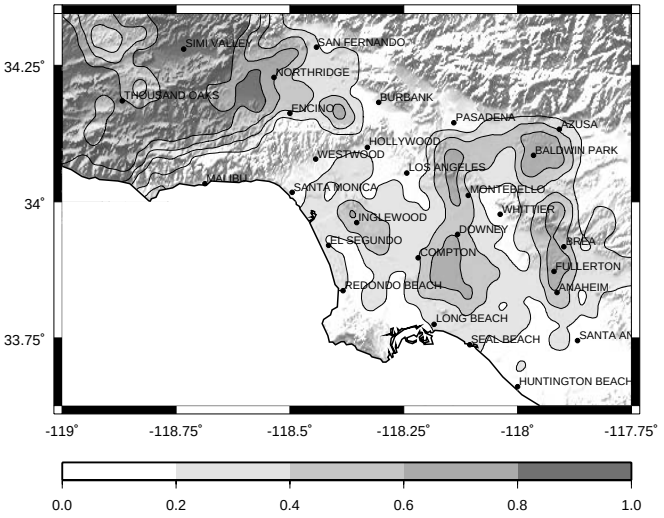

Figure 7. Mean loss for Building 2, normalized by building replacement cost. Compared to Building 1, losses in the Los Angeles basin are significantly lower, but losses in the San Fernando valley remain high.

Figure 8 shows the losses plotted against the residual peak IDR for all 636 analysis sites. It is clear that at higher excitation levels, losses are dominated by the probability of irreparable damage. For Building 1, 309 of the 636 analysis sites have a greater than 50% chance of irreparable damage, while 176 sites for Building 2 fall into that category. Shown in Figure 9 are the losses plotted against the transient peak IDR. We see that for a peak transient of IDR of 0.05, the FEMA acceptance criterion for the collapse prevention (CP) performance level, building losses exceed 50% for much of the region, with near-total losses occurring when the peak IDR exceeds 0.075.

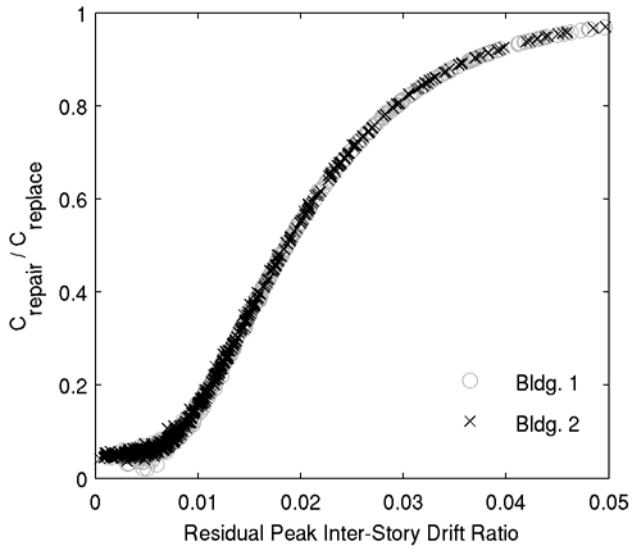

Figure 8. Normalized mean losses for Buildings 1 and 2 plotted against the peak residual inter-story drift ratio (IDR). For values greater than about 0.05, cost is dominated by the probability of irreparable damage, as discussed in Section 3.

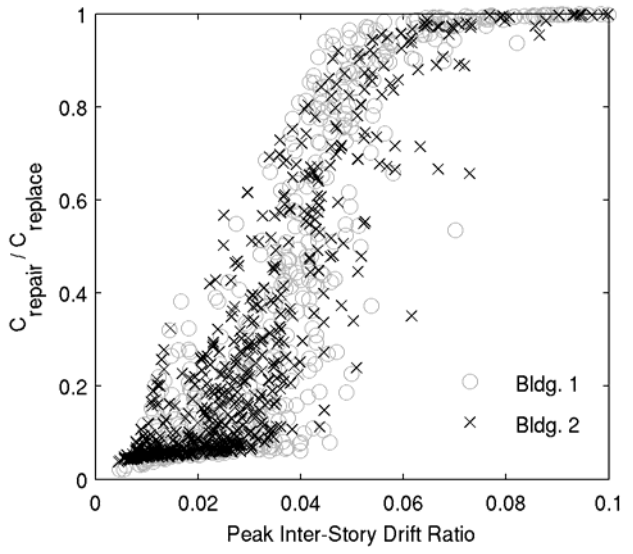

Figure 9. Normalized mean losses for Buildings 1 and 2 plotted against the peak transient IDR. Note that the mean loss for both buildings reaches the replacement cost for peak IDR greater than about 0.075.

5 CONCLUSIONS

In this prototype study, we have laid the framework for performing a quantitative seismic hazard analysis by detailed simulations at all stages: source rupture, seismic wave propagation, structural response, and induced economic loss. The framework allows for effects such as source rupture directivity and slip distribution, both of which play a critical role in determining the intensity of ground motion at a particular site, to be considered. By simulating a large number of plausible earthquakes of varying magnitude from the relevant regional faults and weighing them by their probability of occurrence over a specified time period, it will be possible to develop a more accurate picture of the economic seismic risk faced by a given building. Additionally, by developing a realistic inventory of buildings and other engineered structures, this method can be applied to combine advanced earthquake simulations with structural modeling and PBEE loss methodologies to estimate region-wide losses for major scenario events, which would be very useful in recovery planning.

6 REFERENCES

Bonowitz, & Maison, B. 2003. Northridge welded steel moment-frame damage data and its use for rapid loss estimation. *Earthquake Spectra* 19(3): 335-364.

Carlson, A. 1999. Three-dimensional nonlinear inelastic analysis of steel moment frame buildings damaged by earthquake excitations. Report EERL 99-02, Earthquake Engineering Laboratory, California Institute of Technology, Pasadena, California, USA.

FEMA (2000). Prestandard and commentary for the seismic rehabilitation of buildings. Report FEMA 356. Federal Emergency Management Agency, USA.

Goulet, C., Haselton, C., Mitrani-Reiser, J., Beck, J., Deierlein, G., Porter, K. & Stewart, J., 2007. Evaluation of the seismic performance of a code-conforming reinforced-concrete frame building – from seismic hazard to collapse safety to economic loss. *Earthquake Engineering and Structural Dyn*amics 36: 1973-1997.

Iwata, Y., Sugimoto, H., & Kuwamura, H. 2006. Reparability limit of steel structural buildings based on the actual data of Hyogoken-Nanbu earthquake. *Technical Memorandum of Public Works Research Institute* 4022: 86-95.

Ji, C., Tan, Y., Helmberger, D., & Tromp, J. 2003. Modeling teleseismic P and SH static offsets for great strike-slip earthquakes. In *Proceedings of the American Geophysical Union Fall Meeting*, USA.

Komatitsch, D. & Tromp, J. 1999. Introduction to the spectral element method for three-dimensional seismic wave propagation. *Geophys. J. Int.* 139: 806-822.

Krishnan, S. 2003. FRAME3D – a program for three-dimensional nonlinear time-history analysis of steel buildings: User guide. Report EERL 2003-03, Earthquake Engineering Research Laboratory, California Institute of Technology, Pasadena, California, USA.

Krishnan, S. & Hall, J. 2006a. Modeling steel frame buildings in three dimensions – Part I: Panel zone and plastic hinge beam elements. *Journal of Engineering Mechanics* 132(4): 345-358.

Krishnan, S. & Hall, J. 2006b. Modeling steel frame buildings in three dimensions – Part II: Elastofiber beam elements and examples. *Journal of Engineering Mechanics* 132(4): 359-374.

Krishnan, S., Ji, C., Komatitsch, D., & Tromp, J. 2005. Performance of 18-story steel moment frame buildings during a large San Andreas earthquake – a Southern California-wide end-to-end simulation. Report EERL 2005-01, Earthquake Engineering Research Laboratory, California Institute of Technology, Pasadena, California, USA.

Krishnan, S., Ji, C., Komatitsch, D., & Tromp, J. 2006a. Case studies of damage to tall steel moment frame buildings in southern California during large San Andreas earthquakes. *Bulletin of the Seismological Society of America* 96(4): 1523-1537.

Krishnan, S., Ji, C., Komatitsch, D., & Tromp, J. 2006b. Performance of two 18-story steel moment frame buildings in southern California during two large simulated San Andreas earthquakes. *Earthquake Spectra* 22(4): 1035-1061.

Mitrani-Reiser, J. 2007. *An Ounce of Prevention: Probabilistic Loss Estimation for Performance-Based Earthquake Engineering.* Ph. D. thesis, California Institute of Technology, Pasadena, California, USA.

Moehle, J. & Deierlein, G. 2004. A framework methodology for performance-based earthquake engineering. In *International Workshop on Performance-Based Engineering*, Bled, Slovenia.

Porter, K. 2000. *Assembly-Based Vulnerability of Buildings and its Uses in Seismic Performance Evaluationand Risk-Management Decision-Making*. Ph. D. thesis, Stanford University, Stanford, California, USA.

Porter, K. 2003. An overview of PEER's performance-based earthquake engineering methodology. In *Proceedings of the Ninth International Conference on Applications of Statistics and Probability in Civil Engineering*, San Francisco, California, USA.

Porter, K. 2007. Fragility of hydraulic elevators for use in performance-based earthquake engineering. *Earthquake Spectra* 23(2): 459-469.

SAC. 1995. Analytical and field investigations of buildings affected by the Northridge earthquake of January 17, 1994 – Part 2. Report SAC 95-04, Structural Engineers Association of California, Applied Technology Council, and California Universities for Research in Earthquake Engineering, USA.